

# An ab Initio Study of the Amidic Bond Cleavage by OH<sup>-</sup> in Formamide

Giuliano Alagona, Eolo Scrocco, and Jacopo Tomasi\*

Contribution from the Laboratorio di Chimica Quantistica ed Energetica Molecolare del C.N.R., 56100 Pisa, Italy. Received December 17, 1974

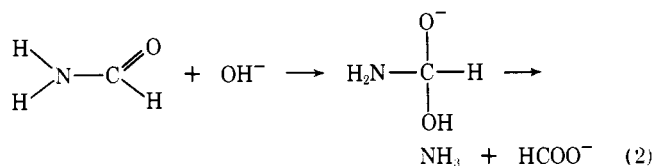
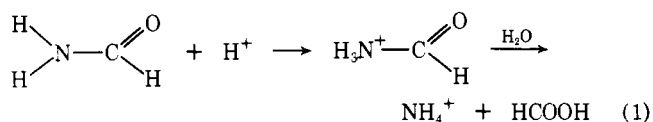
**Abstract:** The mechanism of the reaction  $\text{H}_2\text{NCHO} + \text{OH}^- \rightarrow \text{NH}_3 + \text{HCOO}^-$  in the gas phase has been derived through the determination of the best reaction path on the complete potential surface by ab initio SCF-LCAO-MO calculations. Optimization of practically all the 18 parameters involved leads to the recognition of a stable intermediate with C at an almost tetrahedral hybridization, followed by a barrier corresponding to the transfer of H from O to N. In the STO-3G basis set the intermediate is stable with respect to the reagents of  $\sim 104$  kcal/mol and the barrier height (measured from such intermediate) is of  $\sim 35$  kcal/mol. An analysis of all the changes in geometry along the reaction coordinate and of their contribution to the barrier is also given.

Ab initio calculations of molecular wave functions have reached at present an efficiency sufficient to permit theoretical investigations on the mechanism of the simplest organic reactions. Among these, a good candidate is the acidic or basic hydrolysis of amides, a reaction of some importance in organic and biological chemistry, presumably neither too entangled nor too simple or depleted of theoretical interest.

The theoretical approach however still requires rather drastic simplifications of the reacting system; for instance, it is difficult to describe adequately with ab initio procedures the interactions with the surrounding medium. Moreover, to a mean research team is actually precluded the technique generally adopted in experimental chemistry of getting supplementary information on a given mechanism by perusing the results obtained with different but related reagents.

The best way to overcome such difficulties perhaps consists in getting first a fairly accurate picture for the simplest model, in the present case hydrolysis of the simplest compound, formamide, in vacuo, and deferring to eventual further steps in the investigation the inclusion of the solvent or the examination of the mechanism for more complex compounds in the given family. In such a way, of course, only a very approximate hint to some particular features of the actual reactions can be obtained. In the present case we recall for instance the interesting problem of the hydrolysis of the amidic linkages in polypeptides, where the occurrence of a polymeric chain having a secondary structure surely introduces new features in the mechanism.

The two schemes of acidic and basic hydrolysis of formamide are usually written in the following way:<sup>1</sup>



Recently, an ab initio study on the main features of reaction 1 has been published by Hopkinson and Csizmadia<sup>2</sup> using SCF calculations performed on a contracted gaussian basis set of single  $\zeta$  quality.

In the present paper only reaction 2 (basic hydrolysis of formamide) will be considered. SCF wave functions on gaussian expansions of minimal basis sets of Slater func-

tions will be employed again, but the expansion here adopted (STO-3G<sup>3</sup>) is a little shorter than that employed in the above quoted paper.

When one uses minimal basis sets there is the risk of introducing into the already oversimplified model (absence of the solvent, one-determinant description, etc.) further sources of uncertainty on the reliability of the results. We consider it more profitable, however, to have a coherent and complete picture of the overall mechanism rather than to have more reliable results on a few intuitively selected aspects of the reaction.

The main object of this paper is to present a fairly detailed description of the reaction coordinate sufficient to visualize the optimum geometry variations in the system, from the isolated reagents to the completely isolated products. With such an aim, we have tried to detect, in its essential features, the minimum energy path on the whole potential energy hypersurface. Such a surface has 18 dimensions and its complete determination is practically unreachable (even with a minimal basis!). The determination of the minimum energy path here presented has been obtained, however, through the optimization of a rather generous number of parameters, which will be specified in the course of the description, on fairly large portions of the overall hypersurface.

According to the results, the reaction can be divided in three main steps: (i) approach of OH<sup>-</sup> to formamide, (ii) formation of a stable intermediate, (iii) inner transfer of a hydrogen atom and separation of the products. Such three steps will be examined separately.

## Reagents and Their Approach

For formamide a completely planar structure was selected,<sup>4</sup> with geometry optimized in all the nine parameters. For the optimization of such geometrical parameters, and also for all the other minimizations performed in the course of this work, an iterative technique consisting of optimizing the parameters one by one and repeating such optimization until convergence was followed. The final values of the parameters for formamide (as well as that for OH<sup>-</sup>), and the energy, will be reported in the first column of Table II.<sup>5</sup>

In the first stage of the reaction it is more interesting to have an overall picture of the different channels available for the mutual approach of the reagents rather than a description of a unique reaction path. It is possible in fact that different channels are competitive among them and consequently a description relying upon a single channel may give a substantially inexact idea of the process. In order to get such a picture we have followed a set of three different

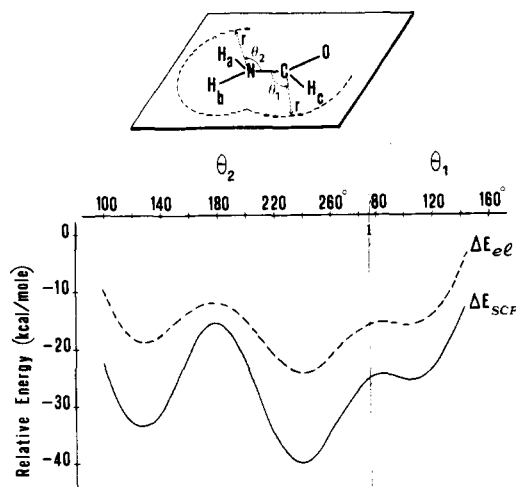


Figure 1. Trend of the interaction energy for angular variations of  $\text{OH}^-$  position in the formamide plane at  $r = 2.5 \text{ \AA}$ . Full line: SCF calculation with fixed internal geometries of the partners. Dashed line: electrostatic calculations.

approximations, mainly to control to what extent it is possible to describe the approach of an ionic reagent with simpler techniques without a substantial loss of information.

At a first stage, when the two partners are still far away, the approximation of using rigid charge distribution for both molecules was employed. The interaction energy is then only electrostatic and may be written as<sup>7</sup>

$$\Delta E_{e1} = \int V_{\text{H}_2\text{NCHO}}(1) \gamma_{\text{OH}^-}(1) d\tau_1 \quad (3)$$

where the first factor of the integrand is the electrostatic potential of the formamide molecule:

$$V_{\text{H}_2\text{NCHO}}(1) = \int \gamma_{\text{H}_2\text{NCHO}}(2) \frac{1}{r_{12}} d\tau_2 \quad (4)$$

the  $\gamma$ 's in (3) and (4) are the overall electronic and nuclear charge density distributions of the molecules.

In the framework of the electrostatic approximation, the charge density distribution  $\gamma_{\text{OH}^-}$  of  $\text{OH}^-$  can be further approximated, without loss of essential information, by a single unit negative point charge. The electrostatic interaction energy takes on then the particularly simple expression:

$$\Delta E_{e1} \approx -V_{\text{H}_2\text{NCHO}}(1) \quad (5)$$

The electrostatic energy is a quantity which derives from the wave function of the isolated molecule, and maps giving the value of  $V$  for selected planes of formamide have been already published,<sup>8</sup> but related to another basis set. For consistency, such calculations have been now repeated using the STO-3G wave function; accordingly the numerical values of  $V$  here employed are a little different from those reported in ref 8, but the shape of the potential is practically the same with the two wave functions.

In this approximation the most favored channels for the approach of  $\text{OH}^-$  lie in the formamide plane, and correspond to the directions of the three X-H bonds.

Electrostatic calculations are in substantial agreement with SCF calculations performed by keeping the internal geometries of the partners unaltered. Such second approximation allows for the mutual polarization effects, the non-classical exchange contributions to the energy, and to some extent the charge transfer effects. The accord between the two approximations is of course better at larger distances, but it is also present at intermediate values of the approach coordinate. Figure 1 gives an example of the quality of this agreement at intermediate distances; for a given distance of

Table I. Energy and Location of the Minimal along the Three Main Channels of Approach of  $\text{OH}^-$  to Formamide, According to the Fixed Geometry Approximation

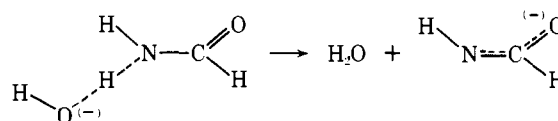
Channels	$R_{\text{opt}}^a$	$\Delta E^b$
$\alpha$ Approach along $\text{NH}_a$	2.49	-34.8
$\beta$ Approach along $\text{NH}_b$	2.40	-40.5
$\gamma$ Approach along $\text{CH}_c$	2.65	-28.2

<sup>a</sup>Distance in  $\text{\AA}$  of O from the heavy atom (N or C) directly interested in the channel. <sup>b</sup>Value in kcal/mol of the interaction energy measured from the isolated reagents.

$2.5 \text{ \AA}$  from the center of mass of  $\text{OH}^-$  to the heavy atom (N or C) more directly interested in the approach, a section of the channel corresponding to angular variations in the plane is given. The full line corresponds to SCF calculations and the dashed one to the electrostatic approximation; in both cases the complete separation of the reagents was taken as zero energy. For the other sections of the potential surface, corresponding to angular variations outside the molecular plane (not displayed here), the comparison between SCF and electrostatic results is of the same quality. It may be concluded that the quite simple electrostatic approximation gives, in this case also, useful information on the approach channels in a rather economic manner.

On the whole, the approximation of keeping the internal geometries of the partners fixed gives three different channels, the importance of which is however different. The first channel, pointing toward the  $\text{NH}_a$  bond (cis with respect to  $\text{C}=\text{O}$ ), is well separated from the others, whereas between the second, pointing toward  $\text{NH}_b$ , and the third, pointing toward  $\text{CH}_c$ , there is only a small ridge, and practically the approach of  $\text{OH}^-$  results possibly in a large range of angles covering the whole region between the  $\text{NH}_b$  and  $\text{CH}_c$  bonds. Finally, one obtains three structures of minimum energy, all corresponding to orientations of  $\text{OH}^-$  on the line of the three XH bonds (see Table I).

Of course the approximation of keeping the internal geometries rigid, though useful at larger distances, cannot be retained at this stage of the reaction. Geometry optimization shows that structure  $\gamma$  of Table I actually corresponds to a saddle point in the overall potential surface rather than to a true minimum because there are no barriers with respect to the structures related to minimum  $\beta$ . In



addition, from structures  $\alpha$  and  $\beta$  one reaches exit channels with separation of products corresponding to another reaction mechanism,<sup>9</sup> which we have investigated no further.

On the other side, it turns out that for a certain angle in the region opposite to the carbonyl (say between channels  $\beta$  and  $\gamma$ ) one finds paths leading to a more stable tetrahedral structure with  $\text{OH}^-$  directly bound to C (see below), which corresponds to a true reaction intermediate. In all this portion of space the interaction energies are always negative but we have not found any path starting from the formamide plane and leading monotonically to the reaction intermediate.

Approaching paths starting from positions placed upon the formamide plane do not present, on the contrary, any barriers. When  $\text{OH}^-$  is at large or intermediate distances the interaction energy is less attractive with respect to the cases where  $\text{OH}^-$  is on the molecular plane at equivalent distances, and a smooth valley on the energy surface without local maxima leads eventually to the tetrahedral intermediate.

Table II. Geometrical Parameters<sup>a</sup> and Energies for the Vertical Approach of OH<sup>-</sup> to Formamide

	Reagents					Stable intermediate
Distances, Å						
CO <sub>b</sub>	∞	3.0	2.0	1.75	1.50	
NC	1.404	1.418	1.462	1.50	1.580	
CO <sub>a</sub>	1.218	1.221	1.255	1.278	1.314	
CH <sub>c</sub>	1.105	1.105	1.116	1.126	1.145	
NH <sub>a</sub>	1.014	1.017	1.019	1.024	1.035	
NH <sub>b</sub>	1.013	1.017	1.019	1.024	1.035	
O <sub>b</sub> H <sub>d</sub>	1.068	1.060	1.025	1.005	0.993	
Angles, deg						
∠NCO <sub>a</sub>	124.23	124.07	117.23	115.04	114.0	
∠NCH <sub>c</sub>	111.48	111.22	108.12	104.04	101.50	
∠NCO <sub>b</sub>		91.44	100.36	103.76	103.97	
∠H <sub>c</sub> CO <sub>b</sub>		88.83	94.34	97.35	102.0	
∠O <sub>a</sub> CO <sub>b</sub>		94.0	104.58	110.19	113.50	
∠CO <sub>b</sub> H <sub>d</sub>		95.65	98.54	100.20	103.60	
∠CNH <sub>a</sub>	120.38	108.96	109.02	107.56	107.55	
∠CNH <sub>b</sub>	121.62	108.96	109.02	107.56	107.55	
∠H <sub>a</sub> NH <sub>b</sub>	118.0	106.54	104.90	103.38	102.02	
Torsion angles						
τ <sub>1</sub> = rNCO <sub>b</sub>		16.11	20.44	24.34	30.0	
τ <sub>2</sub> = NCO <sub>b</sub> H <sub>d</sub>		<i>c</i>	-114.79	-113.97	-111.0	
Extra pyramidalization parameters						
∠rNC	180 <sup>b</sup>	122.91	122.33	119.13	118.64	
∠sCN	180 <sup>b</sup>	175.12	148.01	135.31	127.93	
<i>E</i> , hartrees	-240.7532	-240.7760	-240.8531	-240.8944	-240.9187	
Δ <i>E</i> , kcal/mol	0	-14.3	-62.7	-88.6	-103.9	

<sup>a</sup>For the identification of the atoms see Figure 3a. The torsion angle of the system ABCD is defined as the angle between the plane ABC and BCD; this angle is positive for clockwise rotations of CD around BC when looking from B to C; the value  $\tau = 0^\circ$  corresponds to a planar *cis* arrangement of the system. In  $\tau_1$ , as A was chosen a point on the line *r*, the median of the triangle H<sub>a</sub>NH<sub>b</sub>. <sup>b</sup>The values in italic are not optimized; formamide is assumed to be planar. <sup>c</sup>This rotation is practically free (see text for details).

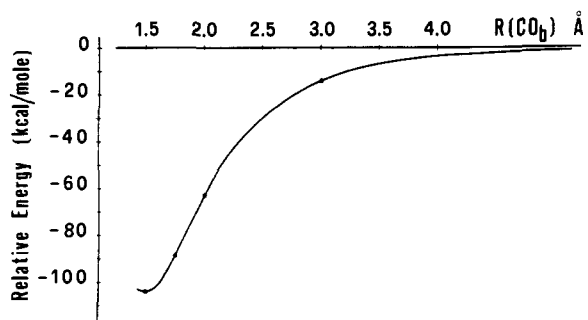


Figure 2. Trend of the interaction energy for vertical approach of OH<sup>-</sup> to formamide.

This energy valley is quite wide for distances C...OH larger than 3 Å and becomes narrower as OH<sup>-</sup> approaches the C atom. In Figure 2 we report the energy profile along the bottom of such a valley (using the C...O<sub>b</sub> distance as guide parameter), and the geometries for some points on this reaction coordinate are reported in Table II. In order to determine the bottom of the valley an optimization of all the geometrical parameters (with the constraints  $R(\text{NH}_a) = R(\text{NH}_b)$  and  $\angle\text{CNH}_a = \angle\text{CNH}_b$ ) was performed at pre-selected  $R(\text{CO}_b)$  values.

By perusing the data of Table II it is clear that the pyramidalization process of the C atom involves changes in all the distances and angles for the atoms directly bound to this atom. The trend of such changes parallels that of the interaction energy displayed in Figure 2. On the contrary the pyramidalization of the N atom, which derives from the disappearance of the conjugation of the p lone pair of the nitrogen with the  $\pi$  molecular orbital of the carbonyl group, is already accomplished at  $R(\text{CO}_b)$  values larger than 3 Å. In

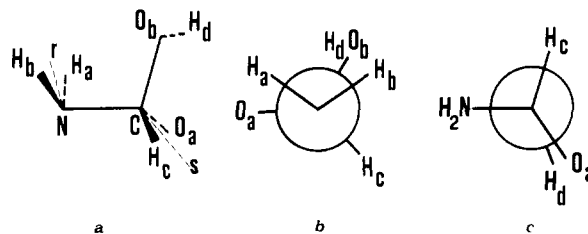


Figure 3. Geometry of the stable intermediate.

order to make easier the appreciation of the tetrahedralization process of the C and N atoms we have added in Table II, as redundant coordinates, the angles  $\angle s\text{CN}$  and  $\angle r\text{NC}$  where *s* and *r* stand for points lying on the median line of  $\angle\text{O}_a\text{CH}_c$  and  $\angle\text{H}_a\text{NH}_b$  triangles respectively (see Figure 3 for the notation of the atoms). For planar arrangements of the relevant atoms such angles are 180° and become 125.26° for a regular tetrahedron.

It may be of some interest to remark the likeness of this picture of the OH<sup>-</sup> approach to formamide to that obtained by Bürgi et al.<sup>10,11</sup> for the addition of H<sup>-</sup> to the formaldehyde molecule using the same method of getting reaction coordinates by means of SCF-MO calculations. At large distances the approach of the nucleophile is favored on the formaldehyde plane, while at distances H<sup>-</sup>...C smaller than 3 Å the approach valley (in this case without intermediate maxima) curves out of the molecular plane and lies on the symmetry plane perpendicular to the H<sub>2</sub>CO molecule. The pyramidalization of the C atom occurs with a trend similar to that found in the present paper, while differences in the two sets of calculations can be easily rationalized if one takes into account that in the case we are discussing now there is a lower symmetry and additional degrees of freedom.

For instance the requirements on the orientation of  $\text{OH}^-$  become more stringent as the nucleophile approaches C: the rotational barrier for  $\text{OH}^-$  at the best  $\angle\text{COH}$  angle is less than 0.8 kcal/mol at 3 Å and becomes 2.8 and 5.9 kcal/mol at 2.0 and 1.75 Å, respectively.

Another feature of the perpendicular approach of  $\text{OH}^-$  to formamide which is of some interest for its implications concerning the mechanism is the value of the angle between  $\text{OH}^-$  and the  $\text{C}=\text{O}$  group  $\angle\text{O}_b\text{CO}_b$  in Table II). Such an angle increases smoothly reaching for the last portion of the approaching path a value around  $110^\circ$ : such a value should be compared with the value of  $98^\circ$  obtained by Storm and Koshland<sup>12</sup> interpreting kinetic data, and with the range  $100\text{--}110^\circ$  proposed by Bürgi et al.<sup>11,13</sup> combining calculations and structural data.

A correlation between the information on the potential energy hypersurface derived by actual calculations and that obtained by interpreting kinetic data concerning the acceleration of intramolecular reactions of nucleophiles at the carbonyl group is not straightforward. As a matter of fact our calculations of the reaction path do not give a dynamical account of the reaction (a statistical analysis over actual trajectories, which depend upon the initial moments of the partners as well as upon the whole energy hypersurface, should be performed) and secondly the kinetic data in question are related to free energies of activation in solution, and it is not simple to interpret entropic and enthalpic factors because the solvent effects can alter the entropic as well as the enthalpic contributions to the free energy along the reaction coordinate. We will return to this topic in the last section of the paper, but we remark here that the reader can find in the already quoted paper of Bürgi et al.<sup>11</sup> a reasonable attempt to correlate the results of an ab initio determination of the reaction path with empirical concepts like togetherness<sup>14</sup> or proximity<sup>15</sup> and orbital steering<sup>15</sup> or orientation effects<sup>12,16</sup> introduced for rationalizing experimental data concerning the intermediate formation.

As a conclusion of this section of the paper one can state that SCF calculations on the supermolecule with geometry optimization show that  $\text{OH}^-$  approach to  $\text{NH}_2\text{CHO}$  will lead to a unique tetrahedral intermediate if  $\text{OH}^-$  starts from positions ranging from the molecular plane (on the side of the CH bond) to the vertical of the N-C axis.

### Reaction Intermediate

The geometrical parameters we have found for the intermediate are reported in the last column of Table II, and a sketch of the geometry is given in Figure 3a.

Notice that the CN bond is notably longer than in formamide while the lengths of the  $\text{CO}_a$  and  $\text{CO}_b$  bonds parallel those found in the  $\text{CH}_2(\text{OH})\text{O}^-$  species (1.355 and 1.477 Å respectively) by Bürgi et al.<sup>11</sup>

The deviations from tetrahedrality of the carbon atom are quite limited in spite of the asymmetry of the substituents at the C atom. It may be of some interest to remark the conformation assumed by the intermediate, because the noticeable amount of information, experimental as well as theoretical, thus far collected about the most stable conformations of similar species has led to several attempts to rationalize data<sup>17-19</sup> which the reader can find interesting to check with the present case. The values of the dihedral angles  $\tau_1 = 30^\circ$  and  $\tau_2 = -111^\circ$  nearly correspond to a trans arrangement of the N lone pair with respect to the  $\text{CO}_b$  group (i.e., the  $\text{CO}_b$  bond is antiperiplanar to the N lone pair) and to a cis arrangement of the  $\text{O}_b\text{H}_d$  bond with respect to the  $\text{CO}_a$  bond (see Figures 3b and 3c).

As said above, this intermediate is strongly stabilized with respect to the reagents ( $\sim 104$  kcal/mol) and it is

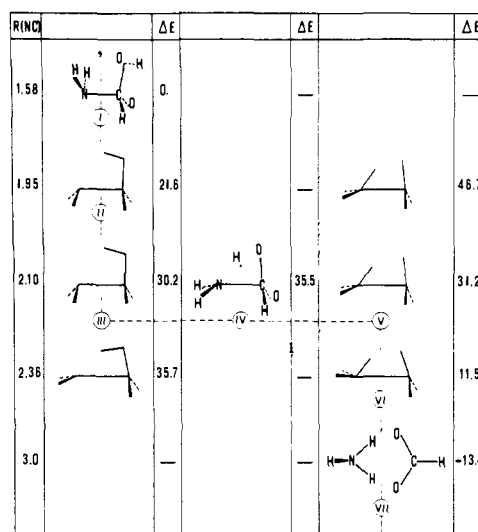


Figure 4. Relative energy and pictorial representation of geometry for some configurations found during the search for the reaction path. Configuration I corresponds to the stable intermediate of Figure 3, configuration IV to the top of the barrier, configuration VII to an adduct of the products. For other information see Table III and the text.

placed at the bottom of a well-defined hole in the potential energy surface.

### Internal Transfer of the Hydrogen and Separation of the Products

The evolution of the system from this intermediate involves practically all the internal coordinates and the determination of the minimum energy path must be performed with great care.

To make clearer the evolution of the system along the reaction coordinate, it is convenient to divide our discussion according to three fundamental steps: (i) conformational variations of the intermediate; (ii) passage of the  $\text{H}_d$  atom from the  $\text{CHOO}$  group to  $\text{NH}_2$ ; (iii) rearrangements of the groups  $\text{NH}_3$  and  $\text{CHOO}^-$ , and their separation. As a guide parameter along the reaction coordinate, the elongation of the NC bond will be used.

A schematic representation of the variations of geometry and energy along a rectified path very near to the true reaction path is given as a dashed line in Figure 4. The configurations reported are all optimized in the geometry and related to the values of the guide parameter  $R(\text{NC})$  reported on the left of the figure, while on the right of each configuration is reported the energy, measured from the stable intermediate. The geometries for configurations indicated by Roman numerals are reported in Table III.

Between configurations I and II there are the conformational changes discussed at the point (i); between configurations III and V there is the passage of  $\text{H}_d$  (point (ii)), while configuration IV corresponds to the top of the barrier (activated complex) with  $\text{H}_d$  about midway between N and  $\text{O}_b$ , finally between V and VII there is the rearrangement of the two groups  $\text{NH}_3$  and  $\text{CHOO}^-$  and the beginning of their separation (point (iii)).

(i) **Conformational Changes.** The conformation of minimum energy described in the preceding section is not the best suited for the transfer of the  $\text{H}_d$  atom and the breakage of the NC bond. The conformational changes correspond to a rotation of the  $\text{O}_b\text{H}_d$  bond, bringing  $\text{H}_d$  in the N-C- $\text{O}_b$  plane and as near as possible to N ( $\tau_2 = 0^\circ$ ), and to a rotation of the  $\text{NH}_2$  group leading the N lone pair in the direction of the  $\text{H}_d$  atom ( $\tau_1 = 180^\circ$ ).

Table III. Geometrical Parameters<sup>a</sup> and Energies for the Decomposition of the Tetrahedral Intermediate

	Reagents	Intermediate configurations						Products
		I	II	III	IV	V	VI	
Distances, Å								
NC	1.404	1.580	1.950	2.10	2.10	2.10	2.36	∞
CO <sub>a</sub>	1.218	1.314	1.250	1.245	1.232	1.249	1.248	1.263
CH <sub>c</sub>	1.105	1.145	<i>1.145<sup>b</sup></i>	<i>1.145</i>	<i>1.145</i>	<i>1.145</i>	<i>1.145</i>	1.149
NH <sub>a</sub>	1.014	1.035	<i>1.035</i>	<i>1.035</i>	<i>1.035</i>	<i>1.035</i>	<i>1.035</i>	1.036
NH <sub>b</sub>	1.013	1.035	<i>1.035</i>	<i>1.035</i>	<i>1.035</i>	<i>1.035</i>	<i>1.035</i>	1.036
CO <sub>b</sub>	∞	1.50	1.451	1.444	1.385	1.318	1.30	1.263
O <sub>b</sub> H <sub>d</sub>	1.068	0.993	0.989	0.988	1.096	1.404	1.423	∞
Angles, deg								
∠NCO <sub>a</sub>	124.23	114.0	112.28	112.05	111.52	107.76	105.10	
∠NCH <sub>c</sub>	111.48	101.50	96.02	93.93	89.47	88.29	92.04	
∠NCO <sub>b</sub>		103.97	93.75	91.35	84.29	82.50	75.30	
∠H <sub>c</sub> CO <sub>b</sub>		102.0	107.51	108.95	112.89	115.48	115.11	114.80
∠O <sub>a</sub> CO <sub>b</sub>		113.50	121.19	121.55	125.40	128.77	130.36	130.40
∠CO <sub>b</sub> H <sub>d</sub>		103.60	99.77	99.77	84.94	81.11	86.94	
∠CNH <sub>a</sub>	120.38	107.55	105.16	104.03	126.61	128.36	128.0	
∠CNH <sub>b</sub>	121.62	107.55	105.16	104.03	126.61	128.36	128.0	
∠H <sub>a</sub> NH <sub>b</sub>	118.00	102.02	100.0	99.0	101.94	103.04	101.62	104.4
Torsion angles								
τ <sub>1</sub> = ∠NCO <sub>b</sub>		30	180	180	180	180	0	
τ <sub>2</sub> = ∠NCO <sub>b</sub> H <sub>d</sub>		-111	0	0	0	0	0	
E, hartrees	-240.7532	-240.9187	-240.8842	-240.8706	-240.8621	-240.8689	-240.9004	-240.9117
ΔE, kcal/mol	0	-103.9	-82.2	-73.7	-68.3	-72.6	-92.4	-99.5

<sup>a</sup> For the identification of the atoms see Figure 3a. <sup>b</sup> The values in italic are not optimized.

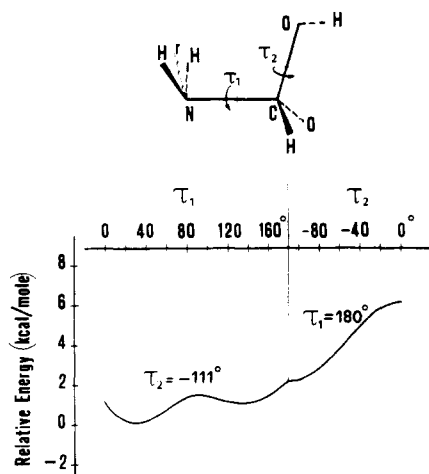


Figure 5. Conformational energy changes in the stable intermediate.

Such changes in conformation along the minimum energy path occur at  $R(\text{NC})$  distances very near to the equilibrium one for the stable intermediate (see Figure 4). To get also an estimate of the conformational energy contribution to the barrier we will report here the results obtained performing all conformational changes just at the equilibrium distance of the intermediate (1.58 Å).

By analyzing the two-dimensional conformation surface in  $\tau_1$  and  $\tau_2$  it was seen that the best path consists in a concerted variation in the intervals  $30^\circ \leq \tau_1 \leq 180^\circ$  and  $-111^\circ \leq \tau_2 \leq 0^\circ$  without barriers and with a loss of energy of 6.2 kcal/mol. In Figure 5 we report the trend of energy for independent variations of  $\tau_1$  (at  $\tau_2 = -111^\circ$ ) and then of  $\tau_2$  (at  $\tau_1 = 180^\circ$ ); the actual path is not very far from this curve.

Because the change of conformation is actually concomitant with some elongation of the NC bond, the above mentioned variation of energy can be considered as an upper limit to the conformational contribution to the reaction barrier.

A fairly extended amount of experimental and theoretical data evidences the role played by the conformation of the tetrahedral intermediate in determining the decomposition route.<sup>20-22</sup> The results of the present investigation show that the most stable conformation does not correspond, at least in this case, to the conformation which actually undergoes decomposition with cleavage of the C-N bond. The changes in conformation we have found seem to be in good accordance with the conclusions reached in ref 22, allowance being made for the differences in the chemical systems considered in the two papers.

(ii) **Transfer of H from O to N.** The lower barrier for the transfer of H<sub>d</sub> was found at  $R(\text{NC}) = 2.1$  Å, a distance decidedly greater than that of the intermediate. The elongation of the NC bond brings the greatest contribution to the barrier, and its value can be estimated to be of the order of 24 kcal/mol, while it may be estimated that the proton transfer contribution to the barrier is less than 5.3 kcal/mol. It should be kept in mind that a separation in single contributions is arbitrary, but it is of some usefulness to appreciate the orders of magnitude related to an eristic picture of the process.

It is worth noticing the change of the  $\angle\text{NCO}_b$  angle, which from the value of  $104^\circ$  for configuration I reaches the value of  $84.3^\circ$  at the top of the barrier (configuration IV). Because of such variation, the distance of H<sub>d</sub> from N decreases slightly in spite of the noticeable elongation of the NC bond. Configurations III and V have been optimized on 13 parameters among the 15 available (see Table III). Assuming as a first approximation for the passage from III to V a linear variation of such parameters, a first determination of the path for the transfer was obtained by calculating the potential surface in the two coordinates defining the position of H<sub>d</sub> in the NCO<sub>b</sub> plane.<sup>23</sup> Then, a new optimization of the 13 geometrical parameters for the configuration at the top of barrier (configuration IV of Table III and Figure 4) was performed. The trend of the energy along the transfer coordinate is reported in Figure 6. The dashed curve refers to the linear approximation of the parameters; the full line was obtained after the optimization of configuration

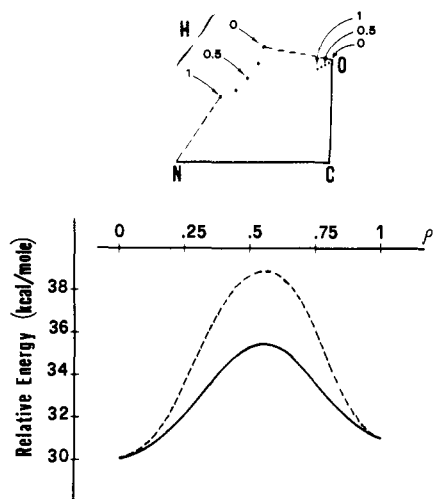


**Figure 6.** Energy profile for the hydrogen transfer. The geometrical sketch at the top of the figure relates the parameter  $\rho$  to the actual transfer path. Dashed line: linear interpolation of the geometrical parameters. Full line: complete optimization.

IV. At the top of this figure the optimum path with the corresponding variations of the position of  $O_b$  is reported; to simplify matters the other atoms have been not drawn.

(iii) **Final Rearrangements and Separation of the Products.** At the top of the barrier the  $NH_3$  group has a structure practically planar, and upon descending it, a process of pyramidalization starts, which continues till the structure of ammonia is reached. The role played by the lone pair of N is worthy of note; in the portion of the path before the barrier it is placed in the half-plane containing also the  $H_d$  atom (see configuration III) and at the time of the hydrogen transfer it is directly involved in the formation of the new bond  $NH_d$ . The weakening of the NC bond due to its elongation involves, after the barrier, the appearance of the nitrogen lone pair in the opposite half-plane.

In the portion of the path which follows barrier, the angle  $\angle NCO_a$  continues to decrease. Other changes in the angles  $\angle NCO_b$  and  $\angle NCH_c$  and distances  $R(CO_a)$  and  $R(CO_b)$  all cooperate in leading the  $CHOO$  group to a planar symmetric structure. At this stage of the reaction it may be noticed how the negative charge becomes progressively more localized on this group which takes on the features of the formate anion.

Immediately after the formation of the two molecules (after configuration VI) interactions between such groups give rise to a reorientation process and to a new minimum on the path. At the bottom of such a minimum a structure characterized by two symmetrical hydrogen bonds of  $N-H\cdots O$  type was found (length  $N-O = 2.71 \text{ \AA}$ , deviation from the linearity =  $23.6^\circ$ ,  $\angle HNH = 97.3^\circ$ ,  $\angle OCO = 129.5^\circ$ ). Such a structure, found with optimization of the parameters involved, is more stable by  $\sim 18 \text{ kcal/mol}$  with respect to the isolated products, whose geometry was also optimized.

### An Overall View of the Reaction Path

Figure 7 which reports changes in energy with respect to the  $R(NC)$  distance may give a concise representation of the reaction path. Curve a is related to structures having the  $H_d$  atom bonded to  $O_b$ , and corresponds to the set of configurations vertically placed on the left side of Figure 4. Curve b is related to structures having the  $H_d$  atom bonded to N and corresponds to the set of configurations vertically placed on the right side of the same Figure 4. Both curves have been obtained by an accurate optimization of the geo-

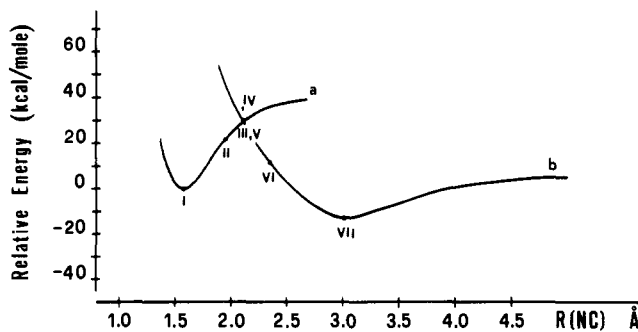


**Figure 7.** Energy profile along the reaction coordinate starting from the stable intermediate I to the products. Point IV is referred to the top of the hydrogen transfer barrier (see Figure 6).

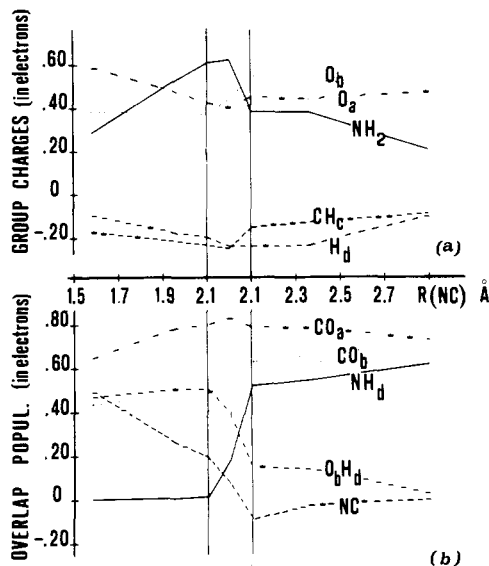


**Figure 8.** Population analysis along the reaction coordinate. The portion of coordinate between the two points at  $R(NC) = 2.1 \text{ \AA}$  corresponds to the transfer of the hydrogen and is somewhat arbitrary in length.

metrical parameters, such as the one shown for configurations I-VII.

At the distance  $R(NC) = 2.1 \text{ \AA}$  both curves a and b correspond to the same energy. The changes in geometry and energy necessary to pass from one curve to the other (and corresponding to the transfer of  $H_d$ ) are related to the set of configurations placed on the horizontal line of Figure 4. As a consequence, if one joins the left portion of curve a to the full line curve of Figure 6 and then to the right portion of curve b, one obtains a one-dimensional representation of the energy profile along the reaction path (slightly rectified near the joint points).

It may be of some interest to report the variations of the total atomic charges and the overlap populations (according to the Mulliken analysis) along such a reaction path (see Figures 8a and 8b). It may be seen that at the top of the barrier there is a change in the derivative of the total charges. The NC bond elongation before the barrier causes a gradual shift of electrons from  $O_a$  toward  $NH_2$ , while during the transfer of  $H_d$  from  $O_b$  toward N one can notice an opposite transfer of electronic charge from  $NH_2$  toward the  $H_cCO_aO_b$  group. After the barrier, when the NC distance increases, such transfer continues until the formation of a formate ion with a unit negative charge. The formation of the  $NH_d$  bond, and the concomitant scission of the other two bonds  $O_bH_d$  and NC, can be easily followed on the overlap population diagram.

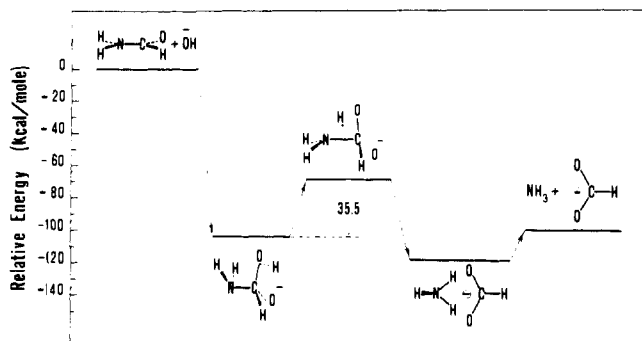


Figure 9. Schematic representation of the reaction profile.

## Conclusions

The picture of the fission of formamide by  $\text{OH}^-$  in the gas phase obtained by means of STO-3G SCF calculations corresponds to a fairly complex mechanism.

The approach of  $\text{OH}^-$ , which is favored in a wide range of solid angles interesting the CH and the NH bond as well as the perpendicular to the C atom, leads to a direct attack on the carbon atom. A neatly stabilized intermediate ( $\sim -104$  kcal/mol with respect to the reagents) follows, and consequently in order to reach the products it is necessary to overcome a barrier ( $\sim +35$  kcal/mol with respect to the intermediate). In the portion of the potential surface corresponding to the products there is another hole corresponding to the formation of an adduct by means of a couple of hydrogen bonds. A schematic representation of the energy profile is given in Figure 9.

The determination of the limits of validity of the results here displayed and of the information which can be derived on the basic hydrolysis of the amidic linkage in general deserves some discussion.

As for the specific case of the reaction of formamide in the gaseous state, the main sources of errors seem to derive from the basis employed in the calculations and from the one-determinant approximation we have assumed. It has been said<sup>24</sup> that STO-3G calculations do not reproduce in an adequate manner the physical situations where bonds are broken and others of different kind are formed. As a matter of fact this is a defect shared by all minimal bases, which, in addition, might be only partially corrected by resorting to double  $\zeta$  bases. A detailed and completely reliable description of the mechanism for such a type of reaction, including also the relevant changes in the correlation energy, hardly seems at present to be a feasible task. We have however the feeling that the main steps in the mechanism (the intermediate and the following barrier) have been approximately identified. Of course upon repeating such analysis with another basis set a different energy of reaction and different ratios between the energies of the most important steps (those of Figure 9, for instance) could be obtained.

If one would try to apply such a mechanism to other amides (still in the gaseous phase), it would be convenient to consider that the substitution of hydrogens with heavier groups would surely alter some aspects of the minimum energy path. The shape of the approach channels would be modified in the regions where an X-H group were substituted by a less reactive group. The last energy minimum, corresponding to an association of the products, would be less deep in all the cases where the substitution did not allow the formation of hydrogen bonds and the interactions would be reduced to polarization effects of the  $\text{RCOO}^-$  anion on the newly formed amine. Other changes are surely possible, depending on the chemical identity of the substitu-

ents, but it is possible that in many cases the sequence intermediate barrier remains unaltered.

Let us consider now the possible effects of an aqueous solvent. It will alter surely, and in rather a drastic manner, the energy profile. Differential effects of solvation along the reaction path will be undoubtedly important. The different dimensions of the charged species suggest that the hydration energy of  $\text{OH}^-$  should be larger than that of the formic anion, and that this product has in turn a somewhat larger solvation stability than the intermediate. Such differences in hydration energies should help in flattening the energy profile. On the whole, if the effects of the solvent were somehow introduced into the model, the energy released by the reaction would be certainly lower, although the experimental value of the hydration enthalpy ( $-6$  kcal/mol<sup>25</sup>) is not likely to be reproduced.

Moreover, the inclusion of the solvent will surely introduce new features on the energy profile. In the initial phase a process of partial desolvation of the reagents should give rise to a barrier preceding the tetrahedral intermediate and also in the final stage of the mechanism here discussed the opposite process of completion of the hydration shells should overcome the formation of the adduct with consequent disappearance of the last minimum we have found on the reaction path. We remember that schematic diagrams of the reaction coordinate vs. free energy on the basis of experimental data are given, for instance, by Guthrie<sup>26</sup> for reactions strictly related to the present one.

The effect of the aqueous solvent could be even more delicate in the intermediate steps of the mechanism; there is the possibility that alternative paths exist, where a water molecule plays an active role.<sup>26-31</sup> From the present calculations no information can be drawn about such alternative paths, and the problem perhaps deserves a further investigation parallel to the present one.

## References and Notes

- See, e.g., (a) A. Liberles, "Introduction to Theoretical Organic Chemistry", Macmillan, New York, N.Y., 1968, pp 585-587; (b) R. T. Morrison and R. N. Boyd, "Organic Chemistry", Allyn and Bacon, Boston, Mass., 1959, pp 481 and 482.
- A. C. Hopkinson and I. G. Csizmadia, *Theor. Chim. Acta*, **31**, 83 (1973).
- W. J. Hehre, R. F. Steward, and J. A. Pople, *J. Chem. Phys.*, **51**, 2657 (1969).
- Formamide is to be considered here a "model" of amide rather than an actual molecule and consequently some particular features of its geometry, i.e., small deviations of N from planarity and asymmetries in the NH bonds, should be regarded as unessential in the present study.
- An independent geometry optimization for formamide, using the same basis set and the same geometry constraint, has been recently published by Dei Bene et al.<sup>6</sup> The good agreement between the two sets of geometrical parameters may be considered as a test of the reliability of the iterative strategy for searching optimum geometries we have adopted.
- J. E. Dei Bene, G. T. Worth, F. T. Marchese, and M. E. Conrad, *Theor. Chim. Acta*, **36**, 195 (1975).
- E. Scrocco and J. Tomasi, *Top. Curr. Chem.*, **42**, 95 (1973).
- R. Bonaccorsi, A. Pullman, E. Scrocco, and J. Tomasi, *Chem. Phys. Lett.*, **12**, 622 (1972).
- See, for instance, ref 1a, p 563.
- H. B. Bürgli, J. M. Lehn, and G. Wipff, *J. Am. Chem. Soc.*, **96**, 1956 (1974).
- H. B. Bürgli, J. D. Dunitz, J. M. Lehn, and G. Wipff, *Tetrahedron*, **30**, 1563 (1974).
- D. R. Storm and D. E. Koshland, *J. Am. Chem. Soc.*, **94**, 5815 (1972).
- H. B. Bürgli, J. D. Dunitz, and E. Shefter, *J. Am. Chem. Soc.*, **95**, 5065 (1973).
- M. I. Page and W. P. Jencks, *Proc. Natl. Acad. Sci. U.S.A.*, **68**, 1678 (1971).
- A. Dafforn and D. E. Koshland, *Biochem. Biophys. Res. Commun.*, **52**, 779 (1973).
- P. Deslongchamps, P. Attani, D. Fréhel, and A. Malaval, *Can. J. Chem.*, **50**, 3405 (1971).
- S. Wolfe, A. Rank, L. M. Tel, and I. G. Csizmadia, *J. Chem. Soc. B*, 136 (1971).
- L. Radom, W. J. Hehre, and J. A. Pople, *J. Am. Chem. Soc.*, **94**, 2371 (1972).
- G. Wipff and H. B. Bürgli, *Helv. Chim. Acta*, **57**, 493 (1973).
- P. Deslongchamps, C. Lebreux, and R. Taillefer, *Can. J. Chem.*, **51**, 1665 (1973).

- (21) P. Deslongchamps, P. Atlani, D. Fréhel, A. Molavai, and C. Moreau, *Can. J. Chem.*, **52**, 3651 (1974).
- (22) J. M. Lehn and G. Wipff, *J. Am. Chem. Soc.*, **96**, 4048 (1974).
- (23) The parameter  $\rho$  ( $0 \leq \rho \leq 1$ ) defining the linear variation of the 13 parameter is related to the rectified distance covered by  $H_1$  along a tentative path determined by means of previous calculations on more rigid geometries. A posteriori it was verified that such a path was substantially correct and very near to that reported in Figure 6. As a consequence it was not considered necessary to start with an iterative series of corrections of the tentative path.
- (24) L. Radom, J. A. Pople, and P. v. R. Schleyer, *J. Am. Chem. Soc.*, **95**, 8193 (1973).
- (25) Data taken from: D. D. Wagman, W. H. Evans, V. B. Parker, I. Halow, S. M. Bailey, and R. H. Schumm, *Natl. Bur. Stand. (U.S.), Tech. Note, No. 270-3* (1968).
- (26) J. P. Guthrie, *J. Am. Chem. Soc.*, **96**, 3608 (1974).
- (27) M. L. Bender and R. J. Thomas, *J. Am. Chem. Soc.*, **83**, 4183 (1961).
- (28) S. O. Eriksson, *Acta Chem. Scand.*, **22**, 892 (1968).
- (29) R. M. Poliak and M. L. Bender, *J. Am. Chem. Soc.*, **92**, 7190 (1970).
- (30) D. Drake, R. L. Schowen, and H. Jayaraman, *J. Am. Chem. Soc.*, **95**, 454 (1973).
- (31) J. M. Sayer and W. P. Jencks, *J. Am. Chem. Soc.*, **95**, 5637 (1973).

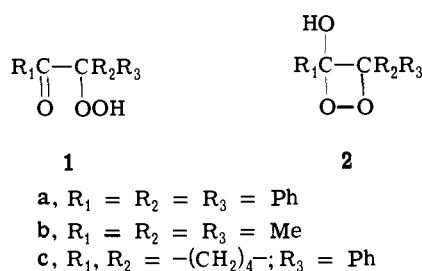
## Kinetics of the Base-Catalyzed Decomposition of $\alpha$ -Hydroperoxy Ketones

Yasuhiko Sawaki and Yoshiro Ogata\*

Contribution No. 215 from the Department of Applied Chemistry, Faculty of Engineering, Nagoya University, Chikusa-ku, Nagoya, Japan. Received March 31, 1975

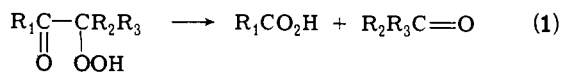
**Abstract:** The alkoxide-catalyzed decomposition of 15  $\alpha$ -hydroperoxy ketones **1a–o** afforded generally high yields of ketones (80–100%) and esters (70–100%). The high yields of esters show that the  $\alpha$ -cleavage reaction proceeds predominantly via an acyclic, carbonyl addition intermediate. The formation of a small amount of carboxylic acid was caused by the reaction of hydroxide ion via the acyclic intermediate rather than via a cyclic 1,2-dioxetane. The pseudo-first-order rate constant,  $k_{\text{obsd}}$ , with respect to **1** is proportional to  $[\text{RONa}]$  at lower base concentrations and then approaches a constant at higher ones. The behavior suggests a reaction between  $\text{RO}^-$  and the undissociated hydroperoxide, and the resulting second-order rate constant ( $k_{10}$ ) for MeONa ranged from  $4.2 \times 10^{-1} \text{ M}^{-1} \text{ sec}^{-1}$  for **1c** to  $5.6 \times 10^{-5} \text{ M}^{-1} \text{ sec}^{-1}$  for **1b** in benzene-methanol at  $0^\circ$ . The substituent effect on  $\alpha$ -hydroperoxy- $\alpha,\alpha$ -diphenylacetophenones exhibited positive  $\rho$  values of 2.5–3.2 and 0.9–1.7 (with  $\sigma$ ) on benzoyl and  $\alpha$ -phenyl rings, respectively. Rate-determining fragmentation of the carbonyl addition intermediate was suggested from the observations: (i) the facile transesterification of  $\alpha$ -hydroperoxy esters (**3**), (ii) the relative reactivities of **1a–n**, and (iii) the effect of hydroxide or hydroperoxide ion on the ester yield.

$\alpha$ -Hydroperoxy ketones are well known as intermediates in the autoxidation of ketones,<sup>1</sup> which were sometimes iso-



lated and identified to be  $\alpha$ -ketohydroperoxide (**1**)<sup>2</sup> rather than 1,2-dioxetane (**2**).<sup>3</sup>

The autoxidation of ketones in basic media rapidly forms  $\alpha$ -hydroperoxy ketones<sup>1d,4</sup> and gives  $\alpha$ -hydroxy ketones in the presence of phosphite.<sup>5</sup> Although  $\alpha$ -hydroperoxy ketones can yield  $\alpha$ -diketones when  $\text{R}_2 = \text{H}$ ,<sup>4d,6</sup> a main alkaline reaction of **1** is the  $\alpha$  cleavage (eq 1).<sup>1d,4,7</sup>



The mechanism was often written to involve 1,2-dioxetane (**2**) or its anion,<sup>1d,7a-f</sup> but an alternative acyclic mechanism was also suggested.<sup>7g-j</sup> Recent studies by Richardson<sup>7f</sup> and by Bordwell<sup>7i</sup> reached two different conclusions, cyclic and acyclic, respectively. We wish to report here our results<sup>8</sup> on the alkaline decomposition of 16  $\alpha$ -hydroperoxy ketones, which support the acyclic mechanism for the  $\alpha$ -carbon cleavage reaction (eq 1) as a main path.

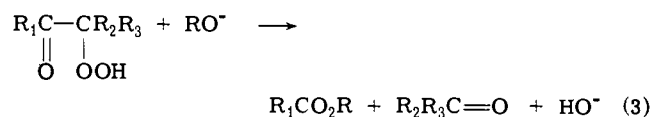
### Results

**Rate.** The reaction of  $\alpha$ -hydroperoxy ketones (**1** or  $\text{R}'\text{OOH}$ ) with sodium alkoxide in benzene-alcohol (1:1 in volume) at  $0^\circ$  was monitored by iodometry and expressed as:

$$v = k_{\text{obsd}}[\text{R}'\text{OOH}] \quad (2)$$

The values of  $k_{\text{obsd}}$  were constant up to 70–80% conversion except at low concentration of alkoxide, where the constancy was observed only at initial 10–20% conversion. The  $k_{\text{obsd}}$  value is proportional to  $[\text{RONa}]$  at  $[\text{EtONa}] < 0.01 \text{ M}$  or at  $[\text{MeONa}] < 0.1$  and then approaches a constant (Table I). The validity of eq 2 at constant  $[\text{RONa}]$  with varying  $[\text{R}'\text{OOH}]$  is also shown in Table IIB. This result, which denies the induced radical decomposition of **1**, together with the high yield of esters (>60%) suggests the unimportance of a base-catalyzed radical decomposition.

**Products.** The reaction of **1a** with alkoxides produced benzophenone and benzoate (Table II).



The yield of the ester decreased at lower  $[\text{RONa}]$  (Tables IIA and IIC) and a small amount of benzoic acid was detected.<sup>9</sup> The addition of water decreased considerably the yield of esters but only slightly the rate of decomposition (Table IIE), which suggests that  $\text{HO}^-$  as well as alkoxide ion can react to form benzoic acid according to eq 3. Ester